Respiratory and cardiac non-rigid motion correction for cardiac PET-MR

Christoph Kolbitsch[1], Mark Ahlman[2], Michael Hansen[3], Javier Royuela del Val[1,4], Peter Kellman[3], David A. Bluemke[2], and Tobias Schaeffter[1]
[1]*Division of Imaging Sciences and Biomedical Engineering, King's College London, London, London, United Kingdom,* [2]*Clinical Center, Radiology and Imaging Sciences, National Institute of Health, Bethesda, MD, United States,* [3]*National Heart, Lung, and Blood Institute, National Institutes of Health, Bethesda, MD, United States,* [4]*Laboratorio de Procesado de Imagen, Universidad de Valladolid, Valladolid, Valladolid, Spain*

INTRODUCTION: Positron emission tomography (PET) is a medical imaging technique commonly used to diagnose and assess ischemic heart disease through myocardial perfusion imaging [1]. The movement of the heart during cardiac and respiratory cycles presents a great challenge to cardiac PET scans leading to image blurring and even signal cancellation [2,3]. Cardiac gating can be used to minimise these motion artefacts but at the cost of longer acquisition time or reduced SNR. Motion compensation techniques using only PET data have been proposed but suffer from poor signal within cardiac phases when split up into a high number of temporal bins and lack of signal contrast inside the myocardium [2].
The recent introduction of clinical simultaneous PET-MR scanners offers the possibility to utilise MR information to correct for motion artefact in the PET images [3-6]. Here we present a MR acquisition using a Golden radial phase encoding (GRPE) sampling scheme [7], which yields 3D high-resolution anatomical MR images and also non-rigid motion information from both the respiration and cardiac function from a single scan. The motion information can be used to compensate for the motion of the heart in both MR and PET images to improve image quality.

METHODS: MR image acquisition (Fig. 1a): MR data was acquired with a GRPE trajectory which yields both high resolution 3D anatomical images and also allows for the reconstruction of dynamic images based on different physiological signals such as a respiratory navigator or an external ECG. This sampling scheme was implemented on a 3T PET-MR scanner (Biograph mMR, Siemens Healthcare) and data was acquired in a patient: T1-weighted GRE (FA 12°, TR/TE 4.7/2.3ms, fat saturation), FOV: 288mm^3 FOV, 1.5mm^3 isotropic resolution after administration of a Gadolinium based blood-pool contrast agent with a total acquisition time of 4.19min.

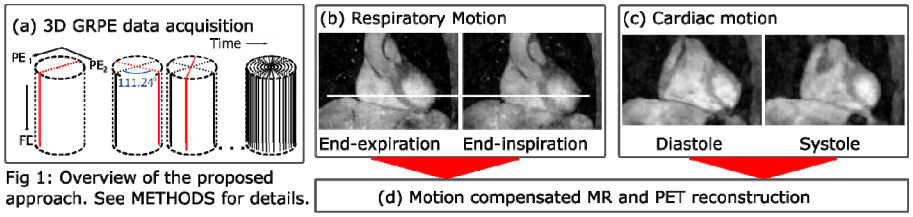

Fig 1: Overview of the proposed approach. See METHODS for details.

Respiratory motion estimation (Fig. 1b): In a first step MR data is binned into 8 respiratory bins using a respiratory self-navigator signal from 1D projections in foot-head direction. 3D images defining different respiratory phases are reconstructed with an iterative non-Cartesian SENSE reconstruction [8] with a total-variation constraint in spatial and temporal direction. Non-rigid motion fields describing the transformation between end-expiration and all other respiratory phases are obtained with a non-rigid registration algorithm [9].
Cardiac motion estimation (Fig. 1c): In a second step the GRPE data is distributed into 10 overlapping cardiac bins based on an external ECG signal. Each cardiac bin covers 125ms. The global translational component of the respiratory motion is corrected prior to image reconstruction by multiplying the k-space data with corresponding linear phase factors. The different cardiac phases are reconstructed using the same algorithm as above. Non-rigid cardiac motion fields are obtained with a non-rigid registration algorithm developed for dynamic data sets [10].
Motion compensated MR image reconstruction: The non-rigid respiratory motion fields are used in a motion compensated MR reconstruction [11] to obtain the final 3D high-resolution anatomical MR image. Cardiac gating based on the ECG is used to minimise artefacts due to cardiac motion.
PET simulation: PET simulations were carried out to study the effect of respiratory and cardiac motion on cardiac perfusion images using STIR [12]. MR images were segmented and the segmentations were transformed to different cardiac and respiratory motion states to simulate realistic physiological motion of the heart. A motion compensated PET image reconstruction (MCIR with ordered subsets expectation maximization (OSEM), 23 subsets, 2 full iterations) with a voxel size of 2mm^3 and 4 mm isotropic 3D Gaussian post-filtering was carried out [12].

RESULTS: Fig. 1b,c shows one slice in different phases of the respiratory and cardiac cycle. The maximum motion amplitude for respiration was 4-6mm at the apex and 6-8mm for cardiac motion along the left ventricle. Fig. 2a shows a reformatted slice visualising the right coronary artery as an indicator of successful motion compensation. For the PET images respiratory and cardiac motion can lead to localised signal drops (Fig. 2b,c black arrow). Nevertheless, the amplitude of both types of motion is similar to the voxel size of the PET images and therefore the image impairment due to motion is very small. Furthermore, the maximum motion amplitude during the cardiac cycle only occurs during a short systolic phase and therefore has little effect on the final image quality.

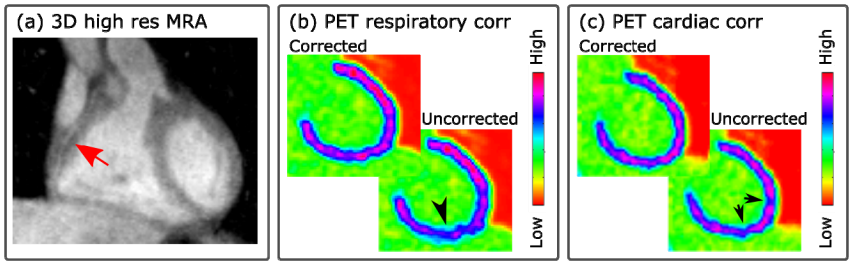

Fig 2: Results for MR (a) and (b,c) PET motion correction

CONCLUSION: We have presented an MR acquisition scheme which provides both 3D high-resolution anatomical information in a very efficient way as well as respiratory and cardiac non-rigid motion information. This information can be used to improve both MR images and simultaneously acquired PET images without an increase in scan time. Future studies to evaluate this approach will be performed to optimise the cardiac motion correction by increasing the number of reconstructed cardiac phases (with a small increase in scan time) and by improving the registration algorithm.

REFERENCES: [1] Di Carli et al., J Nucl Med, 2007:48:783-93. [2] Lamare et al., Med Phys, 2014:41:072504. [3] Petibon et al., Phys Med Biol, 2013:58: 2085-102. [4] Grimm et al., Med Imag Anal, 2015:19:110-20. [5] Würslin et al., J Nucl Med, 2013:54:464-71. [6] Chun et al., J Nucl Med, 2012:53:1284-91. [7] Boubertakh et al., MRM, 2009:62:1331-7. [8] Pruessmann *et al.*, MRM, 2001:46:638-651. [9] Buerger *et al.*, IEEE TMI, 2012:31:805-15. [10] Metz et al., Med Imag Anal, 2011:15:238-49. [11] Batchelor et al., MRM, 2005:54:1273-80. [12] Tsoumpas *et al.*, Phys Med Bio, 2011:56:6597-613.